Influence of bottom topography and mean circulation on large-scale decadal basin modes

Dhouha FERJANI <dhouha.ferjani@univ-brest.fr>,
Thierry HUCK and Alain COLIN DE VERDIERE
Laboratoire de Physique des Océans (UMR 6523 CNRS IFREMER IRD UBO), Brest, France

ABSTRACT

To understand the decadal oscillation which appear in GCMs, we investigate the influence of bottom topography and mean circulation on the propagation and spatial patterns of the linear baroclinic modes of an idealized basin through the linear stability analysis of a two-layer shallow-water model. Various idealized bottom reliefs are analyzed in a rectangular extratropical closed basin mimicking a mid-ocean ridge and/or continental slopes. Only large-scale features are investigated: therefore, eddy effects are parameterized as eddy viscosity and/or thickness diffusion.
The damping of the baroclinic modes is weakly sensitive to the bottom topography. At coarse resolution, it is set by the dissipation. This dissipation selects the largest scale lowest frequency modes as the least damped ones. The low-frequency modes dissipation is rationalized through a detailed energy budgets computed over an oscillation period, and decomposed into barotropic and baroclinic terms, in order to characterize the energy routes and conversions.
With bottom topography, the barotropic mode arises through the interaction of the baroclinic motion with the topography, but this dissipative transfer remains weak with respect to viscous processes. We finally discuss how a mean circulation driven by wind-stress or heat fluxes impact these large-scale modes. In general the modes damping is reduced with increasing mean circulation.

INTRODUCTION

Numerous analysis of historical and climatological time series show significant intrinsic climate variability on interdecadal timescales of the ocean thermocline circulation especially in the Atlantic. The Atlantic Multidecadal Oscillation has been described both in observations and in a hierarchy of ocean models, from quasigeostrophic (QG), shallow water (SW), to planetary geostrophic (PG) and primitive equations (PE) models (Delworth and Mann 2000), as ROMS and HYCOM (see Poster Huck, et al. XY393 in the same session).

On such timescales, the ocean circulation is likely a major player, given its large heat capacity and long adjustment. The latter is achieved through the baroclinic planetary waves that cross the Atlantic basin in a few decades at mid-latitude. Hence interdecadal variability has been linked to baroclinic basin modes, which structure has been investigated in various dynamics and configurations (Ben Jelloul and Huck, 2003, 2005).
The emergence of low-frequency basin modes in reduced-gravity QG and SW dynamics stems from the mass conservation laws and was found to rely both on baroclinic Rossby waves propagation across ocean basins and their interaction with Kelvin boundary waves (Cessi and Primeau 2001, Primeau 2002, Yang and Liu, 2003).

We pursue here these investigation by considering the influence of a background mean circulation and bottom topography on the generic property of the decadal oscillations as well as their damping. The spectrum of baroclinic basin modes has been already investigated in two-layer wind-driven quasi-geostrophic model, the baroclinic basin modes being advected by a barotropic steady flow on top of a flat bottom (Spydell and Cessi 2003, Ben Jelloul and Huck 2005). In the large-scale limit, i.e. for basin scale considerably larger than the Rossby radius of deformation, all the basin modes are neutral. Numerical investigations lead to three types of modes arising for wind forcing strong enough to produce closed geostrophic contours: classical Rossby basin modes deformed by the mean flow (shadow modes), stationary modes and recirculating pool modes, the two latter trapped in the closed-contours pool. Recirculating modes would have very low frequencies for moderate recirculating gyre.
This work is extended here to the shallow water equations, with two active layers on top of various idealized bottom topography (bowl, ridge).The mean circulation is either prescribed in the form of a Sverdrup flow in the case of a double-gyre Ekman forcing and a purely baroclinic flow in the case of a heat flux forcing, or obtained through the integration of the nonlinear model. The equations are linearized for perturbations and the eigenanalysis of the Jacobian matrix is performed in order to provide the modes structure, frequency, and decay rate (figure 1).

THE 2-LAYER SHALLOW WATER MODEL

The basic hypothesis of the shallow water (SW) model is to assume that the active layers are vertically homogeneous and hydrostatic. We consider here a 2-layer SW model in a closed rectangular basin $\Omega = (0 \le x \le Lx\ ,\ -Ly/2 \le y \le Ly/2)$ described in a Cartesian beta-plane centered at 45°N. Nonlinear advection is neglected in the planetary geostrophic approximation. The governing partial differential equations are :

$$\partial_t \mathbf{u_i} + fk \times \mathbf{u_i} = -\nabla p_i + \nu \nabla^2 \mathbf{u_i} + (2-i)\frac{\tau}{\rho_0 h_i}$$
$$\partial_t hi = -\nabla \cdot (h_i \mathbf{u_i}) + (-1)^i S_0$$

where $\mathbf{u}_i=(u_i,v_i)$, $i=1,2$ are the horizontal velocities in the upper and lower layer of thickness h_i and density ρ_i, p_i the pressure: $p_1=g(h_1+h_2+b)$ and $p_2=g(\rho_1/\rho_2\ h_1+h_2+b)$, b the bottom topography above the flat bottom. Dissipation is parametrized through a laplacian eddy viscosity ν appropriate for scales larger than the deformation radius. This form of dissipation parameterizes the effect of the sub-grid scale eddies that are not resolved thus, to avoid grid point structures and isolate large-scale modes through their lower damping rate. We use lateral no-slip boundary conditions everywhere (i.e. no normal flow is allowed through the boundaries).

Forcing: For the wind-driven case, a steady zonal wind stress with a sinusoidal profile $\tau^x(y) = -\tau_0 \cos(2\pi\ y/Ly)$ is used, driving a double gyre. For the buoyancy driven case, the surface heat flux is introduced through interfacial vertical velocities S_0 as a linear function of latitude, corresponding to 40 W/m^2 at the southern boundary and -40 at the northern one. Here, we investigate only one type of forcing at a time.

Topography: We eventually consider two idealized topographic profiles:
- a Mid-Ocean Ridge (R) with a gaussian shape in the x-direction centered in the middle of the basin (that we expect to disturb Rossby waves westward propagation), with a width around one third of the basin extent and an amplitude varying between 0 and 2000 m. The bottom depth is adjusted such that the basin volume remains constant.
-a bowl-shaped topography (labelled C as continental rises).

Stationary solution: The model equations are discretized on an Arakawa C-grid to compute transient flows, time integration uses a leapfrog scheme damped with a three-point Asselin filter (Δt=130 s). The model is integrated for 40 years from an initial flat-interfaces state and reaches a steady-state.

Perturbation: The linear stability analyses are then performed on these steady states, solving an eigenvalue problem of the form : $A\ X = \omega\ X$, where A is a nonsymmetric matrix. The eigenvalue problem is solved using the Arnoldi method as provided in ARPACK (Le houcq et al. 1998) for a prescribed number of eigenvalues (typically 30) selected on the largest real part.

Typical parameters: $Lx = Ly = 6000$ km, $f_0=10^{-4}\ s^{-1}$, $\beta=1.6 \times 10^{-11}\ m^{-1}\ s^{-1}$, H1=1000 m, H2=3000 m, $g_0=9.81\ m\ s^{-2}$, $g'=0.02\ m\ s^{-2}$, $\nu = 10^5\ m^2\ s^{-1}$.

EFFECT OF TOPOGRAPHY ON THE FREE BASIN MODES

The evolution of the global properties of the SW model are addressed through the energy budget of the model to isolate and identify the role of each term on the spin up and decay of the large-scale baroclinic basin dynamics :

$$KE = \frac{1}{2}\rho \int_D h(u^2+v^2)\,dx\,dy\ ,\ APE^+ = \frac{1}{2}\rho_0 g \int_D \eta_1^2\,dx\,dy\ ,\ APE^- = \frac{1}{2}\rho_0 g' \int_D \eta_2^2\,dx\,dy$$

η_1,η_2 are the dynamic topographies i.e. the surface elevation and the vertical displacement of the interface between the two layers.The interaction between the baroclinic modes and the bowl-shaped topography produces a barotropic circulation twice more energetic than the one obtained in the presence of a mid-ocean ridge : around 10% (25%) of the kinetic energy of the least damped baroclinic mode is converted into barotropic one under the effect of 1500m high Ridge (Continental rise) topography (figure2).

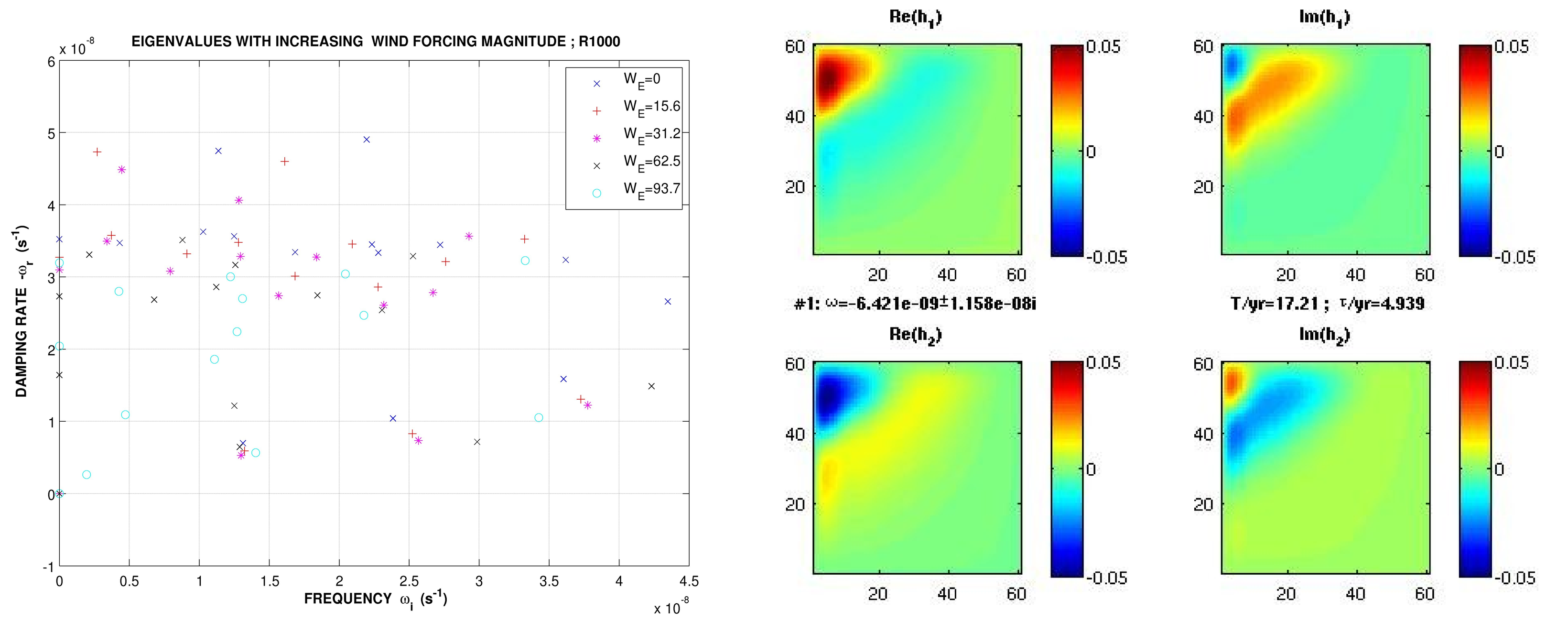

Figure 1 : (left) Eigenvalue spectrum under increasing wind forcing magnitude. (right) Spatial structure of the least damped baroclinic mode labelled N60-R0 in the two layers. The temporal evolution is $Re(h_1,h_2)$--> $-Im(h_1,h_2)$--> $-Re(h_1,h_2)$--> $Im(h_1,h_2)$ for a positive eigenvalue.

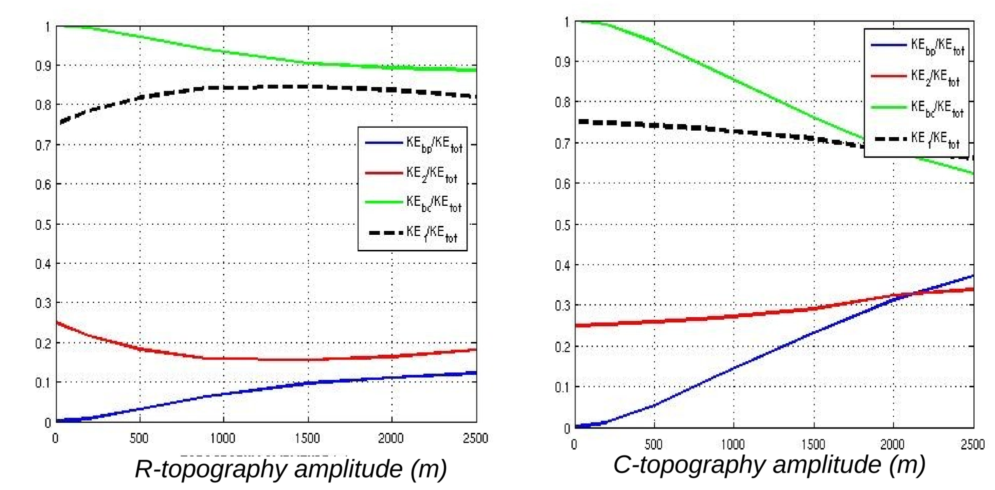

Figure 2: Vertical partition of the kinetic energy ratios of the first least damped basin mode for the two topographic configurations.

The barotropic energy equation reads $\frac{1}{2}h\partial_t \mathbf{u}^{+2} + \frac{1}{2}g\partial_t\eta_1^2 + g'\frac{h_2}{H}\eta_2\partial_t\eta_1 = -\nabla\cdot(p^+ H\mathbf{u}^+) - \frac{g'H_1}{H}\eta_2\,\mathbf{u}^+\nabla b + D^+$

The baroclinic energy equation reads : $\frac{1}{2}\frac{H_1 h_2}{H}\partial_t \mathbf{u}^{-2} + \frac{1}{2}g'\partial_t\eta_2^2 = -\nabla\cdot(\frac{H_1 h_2}{H}p^-\mathbf{u}^-) - g'\eta_2\nabla\cdot(h_2\mathbf{u}^-) + D^-$

The JEBAR term appears in the barotropic energy equation under the form of the second rhs term and has roughly the same order of magnitude and the opposite sign as the baroclinic forcing (the second rhs term in the baroclinic energy equation) in the topographic case.

In the evolution equation for the baroclinic mode, the latter is the coupling term with the barotropic mode. In order to gain further insight into the energy conversion between the two modes, we seek to understand when this latter term acts as a source or sink of energy for the baroclinic mode. with the different variable bottom configurations, the coupling term is seen to act as a sink of energy where the bottom slope is positive that is east of the ridge and in northern part of the continental rises and a source where the bottom slope is negative (figure 3). We note as well that in the sink region, the phase lines of the coupling term are nearly parallel to f/H contours suggesting that the energy conversion occurs preferably along these contours. Overall, the sink is greater than the source, suggesting that the coupling term contributes to dissipate the baroclinic mode.

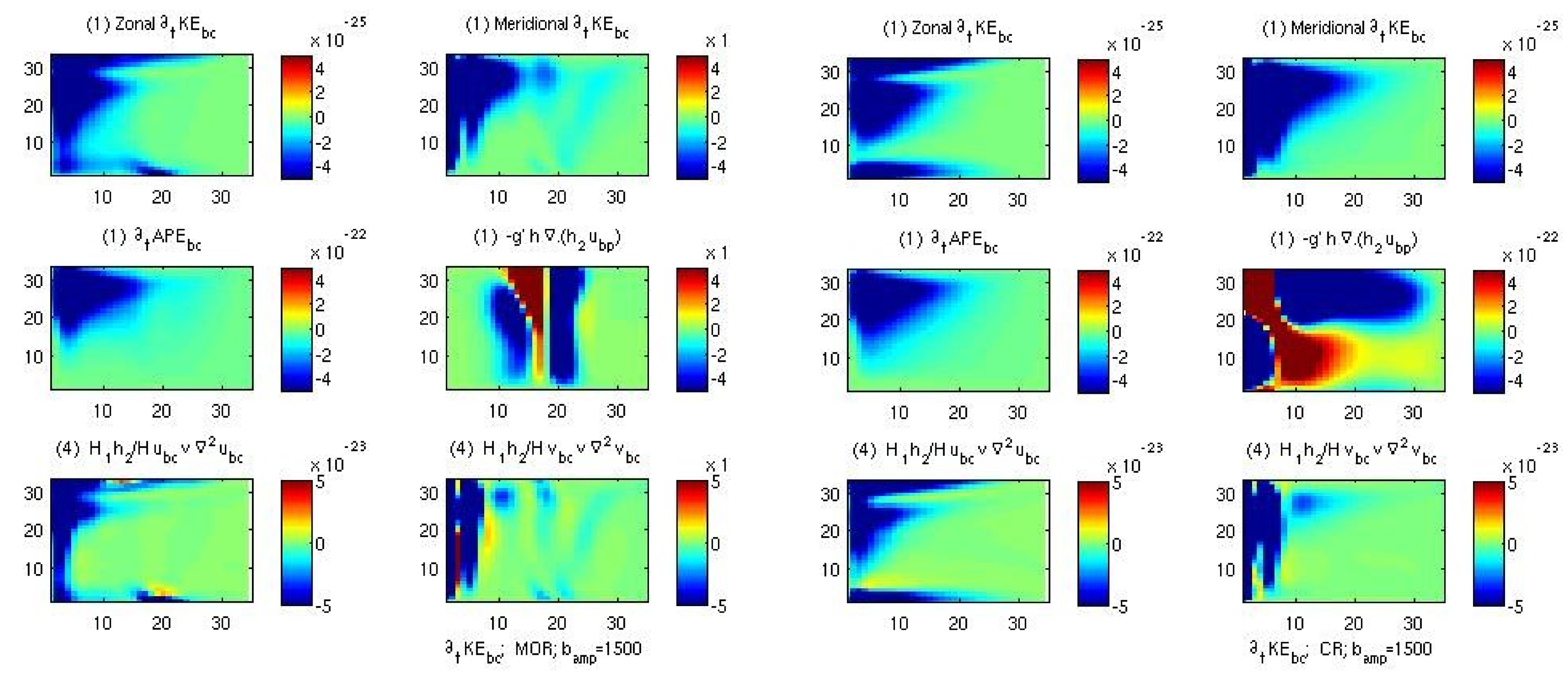

Figure 3 : Baroclinic energy budget with different bottom configurations. (left) In the presence of 1500m-height ridge topography. (right) In the presence of 1500m-height bowl-shaped topography.

BACKGROUND MEAN CIRCULATION

Steady states are computed using increasing forcing magnitude of τ_0 and S_0 as a control parameters with τ_0 and S_0 varying between 0 and 62.5 m/yr and 0 and 31.5 m/yr respectively (figure 4). As pointed out by Sakamoto and Yamagata (1996) and confirmed numerically here, the double gyre Ekman steady state is the same as that of the flat bottom ocean. This is because the wind stress acts only on the upper layer like a body force and there is no mechanism to generate steady currents in the immiscible lower layer. This contrasts with the heat flux forcing that acts equally in the two layers (figure 5). The response of the mean circulation to the two types of forcing suggests that the wind is more efficient in driving the ocean thermocline circulation on interdecadal timescales.

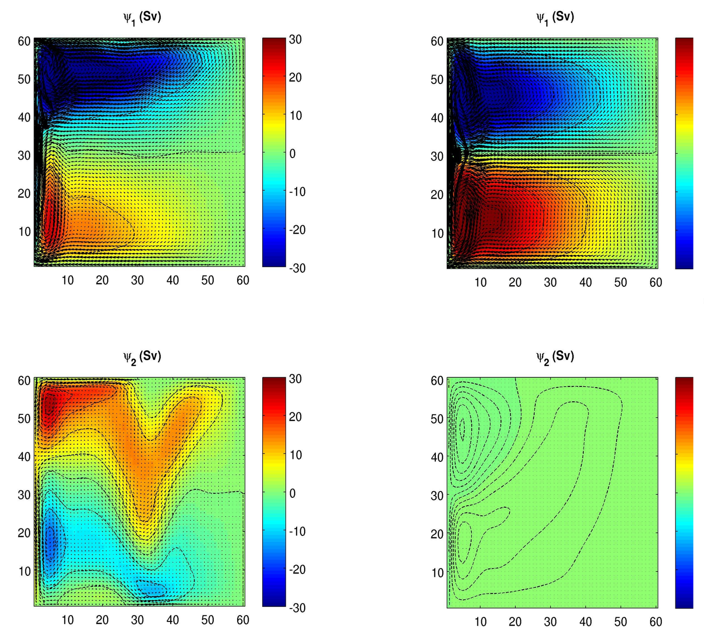

Figure 4: Transport streamfunctions in the upper and lower layer. Left: in a buoyancy-driven circulation of 31 m/yr magnitude +1000m-MOR. Right: in a wind-driven circulation of 0.1 N/m^2 amplitude+Flat.

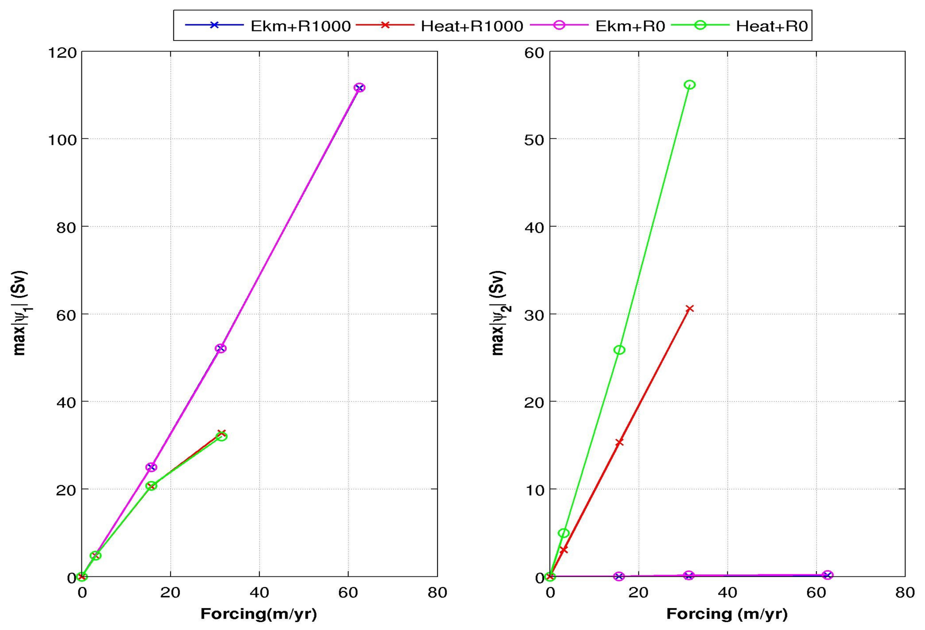

Figure 5: Basin integrated transport streamfunctions as function of increasing forcing amplitude.

EFFECT OF THE BACKGROUND MEAN CIRCULATION ON BASIN MODES

At each magnitude of the forcing, the stability analysis provides the frequency, decay rate and spatial pattern of the modes that perturbs the steady state. A fundamental result is that, depending on the forcing strength, the eigenspectrum displays different behaviors of the basin modes. Note the emregence of a new branch at high forcing magnitude corresponding to a new class of basin modes trapped in closed contour pools (figure 1 left) as reported by Spydell and Cessi (2003) and Ben Jelloul and Huck (2005).

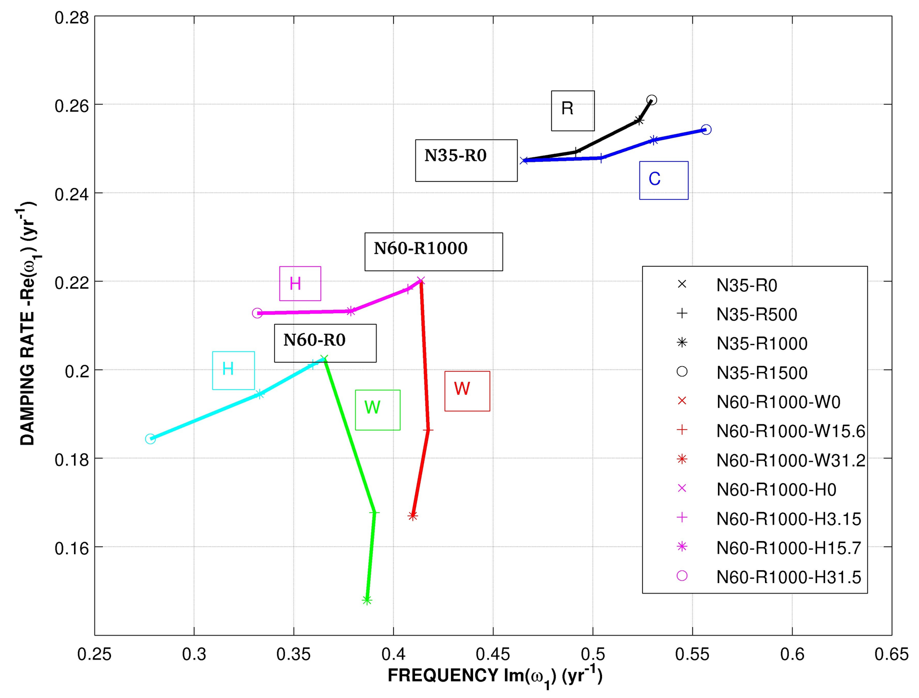

Figure 6: Least damped eigenvalue branching diagram as function of the amplitude of the topography and the two types of mean background circulation. The decay time is reduced with increasing mean flow.

DISCUSSION AND CONCLUSION

Introducing various bottom topography, bowl-shaped or mid-ocean ridge of varying amplitude, did not fundamentally impact the large-scale low-frequency basin modes in a 2-layer shallow water model.
Because of the relatively 'numerically costly' linear stability analysis, we were limited to low resolution, hence large eddy dissipation, either viscosity and/or diffusivity, was required. The topographic dissipation through mode coupling of the linear free perturbations around the rest is found to be weaker compared to the effect of viscous and diffusive decay at first order even with large amplitude topography. At higher resolution though, this might no longer be the case with reduced eddy dissipation coefficients.

With the addition of a mean circulation, either wind or buoyancy forced, the basin modes show reduced damping. No dramatic transition was found for the realistic forcing amplitudes we used. With a climatological forcing, it was expected to find the pool modes as it was the case in 2-layer flat ocean QG model. Surprisingly, such modes were absent in both types of forcing. Pushing up by a factor of 2 the wind forcing allowed to close mean geostrophic contours in the north-west corner and develop a new class of "pool modes".

This work will be extended to three vertical layers to better resolve the stratification to provide the interdecadal mode signature in the North Atlantic.

REFERENCES

Ben Jelloul, M., and T., Huck, 2003: Basin-mode interactions and selection by the mean flow in a reduced-gravity quasigeostrophic model. J. Phys. Oceanogr., 33, 2320-2332.
Ben Jelloul, M., and T., Huck, 2005: Low-frequency basin modes in a two-layer quasigeostrophic model in the presence of a mean gyre flow. J. Phys. Oceanogr., 35, 2167-2186.
Cessi, P., and F. Primeau, 2001: Dissipative selection of low frequency modes in a reduced-gravity basin. J. Phys. Oceanogr., 31, 127-137.
Colin de Verdière, A., and R., Tailleux, 2005: The interaction of a baroclinic mean flow with long Rossby waves. J. Phys. Oceanogr., 35, 865-879.
Huck, T., A., Colin De Verdière, and D. Ferjani, 2012: Multidecadal oscillations of the meridional overturning circulation in the presence of bottom topography. (see poster XY393 in the same session).
Lehoucg, R. B., D. C., Sorensen, and C. Yang, 1996:ARPACK user's guide. Solutions of large scale eigenvalue problems with Implicitly Restarted Arnoldi Methods. SIAM, 160pp. http://caam.rice.edu/software/ARPACK/
Primeau, F. W., 2002: Long Rossby wave basin-crossing time and the resonance of low-frequency basin modes. J. Phys. Oceanogr., 32, 2652-2665.
Sakamoto, T., and T., Yamagata, 1996: Wind-driven ocean circulation. J. Mar. Res. 54, 261-284.
Spydell, M. and P. Cessi, 2003: Baroclinic modes in a two-layer basin. J. Phys. Oceanogr., 33, 610-622.
Tailleux, R. and J.C., McWilliams, 2000: Acceleration, creation, and depletion of wind-driven baroclinic Rossby waves over an ocean ridge. J. Phys. Oceanogr., 30, 2186-2213.
Yang, H., and Z. Liu, 2003: Basin modes in a tropical-extratropical basin. J. Phys. Oceanogr., 33, 2751-2763.\\